

PACS: 71.20.Ad

A.I. Chroneos¹, G. Busker¹, I.L. Goulatis², R.V. Vovk², A.A. Zavgorodniy²,
M.A. Obolenskii², A.G. Petrenko³, V.M. Pinto Simoes^{4,5}, A.V. Samoilov²

ATOMISTIC STUDIES OF Li⁺ MIGRATION IN Y₂O₃ AND THE STRUCTURE OF RELATED OXIDES

¹Department of Materials, Imperial College
London SW7 2BP, United Kingdom
E-mail: chroneos@imel.demokritos.gr

²Kharkov National University
4 Svoboda Sq., 61077 Kharkov, Ukraine

³Donetsk National University
24 University St., 83055 Donetsk, Ukraine

⁴IPA_ Instituto Superior Autónomo de Estudos Politécnicos
Rua de Xabregas, 20, 1º 1900-440 Lisboa, Portugal

⁵Instituto Superior Dom Afonso III
Convento Espirito Santo, 8100-641 Loule, Portugal

Received September 2, 2009

Atomistic computer simulation techniques based on energy minimization have been employed to predict the equilibrium lattice parameters and volumes of a series of rare-earth sesquioxides and their polymorphs. The results have been found in agreement with experimental data and ab initio studies given in the literature. To demonstrate the applicability of the computational methodology the migration of lithium ions (Li⁺) in yttria (Y₂O₃) has been considered.

Keywords: atomistic simulation, crystal structure, lithium migration, rare-earth compounds

1. Introduction

The material properties of rare-earth oxides have been studied extensively because of their wide range of possible applications. For instance, recent experimental studies report the doping of thallium-based cuprate superconductors with rare-earth oxides [1], the beneficial addition of a mixture of rare-earth oxides into molybdenum which enhances the emission properties of cathodes [2] and the unique combination of mechanical, chemical and optical properties of glasses based on rare-earth oxides and alumina [3]. Notably, rare-earth oxides have been

under investigation as potential scintillator materials since they undergo thermoluminescence [4]. Many experimental structural determinations of the rare-earth oxides in the lanthanide series have been carried out for the three distinct polymorphic forms: *A*-type hexagonal (space group $P\bar{3}m1$) [5–9], *B*-type monoclinic (space group $C2/m$) [5,10–12] and *C*-type cubic (space group $Ia3$) [5,13–17]. Density functional theory calculations have also been employed to determine the lattice parameters of a number of rare-earth sesquioxides [18]. The hexagonal *A*-type rare-earth sesquioxides have been initially studied by Zachariasen [19] but the space group $P\bar{3}m1$ has been determined by Pauling [20]. The monoclinic *B*-type has been presented by Cromer [21] as an intermediate form between the low-temperature cubic and high-temperature hexagonal phases.

The purpose of this study is to systematically model these materials using a set of transferable interatomic potentials and compare the resulting structures to the existing experimental [5–17] and theoretical [18] data. The atomistic simulation techniques used here have proved to produce reliable results in previous studies of Y_2O_3 sesquioxide [22–24] and a range of bixbyite materials [25] and indeed many other systems (for example hydroxides [26,27]) beyond the scope of this study. The migration of lithium Li^+ ions in yttria (Y_2O_3) has been considered to illustrate the applicability of the potential models to problems of technological interest.

2. Theoretical methodology

2.1. Simulation technique

The atomistic simulation package GULP [28] was used throughout this study. The simulation technique is based upon a description of the lattice in terms of effective potentials. The Coulomb forces are summed using Ewald's method [29], whereas the short-range forces were modeled using parameterized pair potentials described later. The simulation commences with a perfect lattice calculation where the total energy of the lattice is minimized with respect to the unit cell lattice vectors and the positions of the ions within the unit cell.

This study is based on the classical Born model description of the lattice. The short-range energy terms $S(r_{ij})$ are approximated by a parameterized pair potential of the Buckingham form

$$S(r_{ij}) = A_{ij} \exp\left(-\frac{r_{ij}}{\rho_{ij}}\right) - \frac{C_{ij}}{r_{ij}^6}$$

where r_{ij} is the separation between ions i and j , A_{ij} , ρ_{ij} and C_{ij} are the potential parameters specific to ions i and j . The parameters used in this study were fitted empirically to the experimental lattice parameters and atomic positions of a range of oxide compounds. Essential to this atomistic simulation methodology are parameterized short-range potentials. The potentials used for this study are presented in Table 1 and were derived using the multi-structure fitting procedure described elsewhere [22–25]. The oxygen ions are treated as polarisable by virtue of the

Dick and Overhauser shell model [30]. The O^{2-} ions have a shell charge of $-2.04 |e|$, a core charge of $0.04 |e|$ and a force constant $6.3 \text{ eV} \cdot \text{\AA}^{-2}$.

Table 1

Short-range interatomic potential parameters

Interaction	$A, \text{ eV}$	$\rho, \text{ \AA}$	$C, \text{ eV} \cdot \text{\AA}^6$
$O^{2-}-O^{2-}$	9547.96	0.2192	32.0
$La^{3+}-O^{2-}$	2078.5	0.3467	15.55
$Ce^{3+}-O^{2-}$	20.15.3	0.3437	15.9
$Pr^{3+}-O^{2-}$	2004.6	0.3415	14.2
$Nd^{3+}-O^{2-}$	1975.2	0.3404	13.8
$Sm^{3+}-O^{2-}$	1941.9	0.34	12.55
$Eu^{3+}-O^{2-}$	1888.6	0.34	12.2
$Gd^{3+}-O^{2-}$	1855.9	0.339	11.9
$Tb^{3+}-O^{2-}$	1838.2	0.3385	14.5

In order to simulate the effect of a defect, the lattice is subsequently partitioned into concentric spherical regions according to the Mott–Littleton procedure [31]. The lattice is relaxed around the defect as energy minimization proceeds. It is important to select large enough region sizes so as no significant change in defect formation energy occurs if the region sizes are increased further. In these calculations region I had a radius of 10 \AA (456 species) and region IIa extends the radius to 31 \AA (13000 species).

2.2. Migration Enthalpy Calculation

The static atomistic simulation code was applied to predict defect enthalpies of intermediate steps in migration mechanisms. In Y_2O_3 activated migration mechanisms consist of sequential jumps of the migrating ions between interstitial sites. Y_2O_3 exhibits the cubic C -type rare-earth sesquioxides (bixbyite structure, space group $Ia3$) with a lattice parameter of 10.604 \AA [32]. The bixbyite structure can accommodate interstitial ions at three distinct sites: the $8b$ position, the $16c$ ($x = 1/8$) position and the $24d$ ($x = -1/4$) position. The activation enthalpy for migration is the difference between the enthalpy of the system when the migrating ion is at the saddle point and the enthalpy of the ion at equilibrium. The saddle point enthalpy is calculated by introducing a fixed lithium ion at the saddle point location and then relaxing the surrounding lattice. The evaluation of the potential energy surface both parallel and perpendicular to the diffusion path is necessary to identify the configuration of the diffusion path.

3. Results and Discussion

3.1. Basic Lattice Properties

Before simulating the effect of defects in the rare-earth oxides it is necessary to simulate the structural properties and compare them to the corresponding experi-

mental data. The experimental [10–12] structural parameters of the *B*-type rare-earth sesquioxides are presented in Table 2 and compared with the atomistic simulation data shown in Table 3. The energy minimized volumes of *B*-type monoclinic Sm_2O_3 , Eu_2O_3 and Tb_2O_3 are overestimated by less than 1.4%. To elucidate trends, the volume per molecule (stoichiometric formula unit) of *A*-type and *C*-type rare-earth sesquioxides were compared in Fig. 1 and Fig. 2, respectively. The atomic scale simulations results for the *A*-type rare-earth sesquioxides are significantly closer to the experimental results than the *ab initio* data, apart from the case of La_2O_3 , which is overestimated by 1.4%.

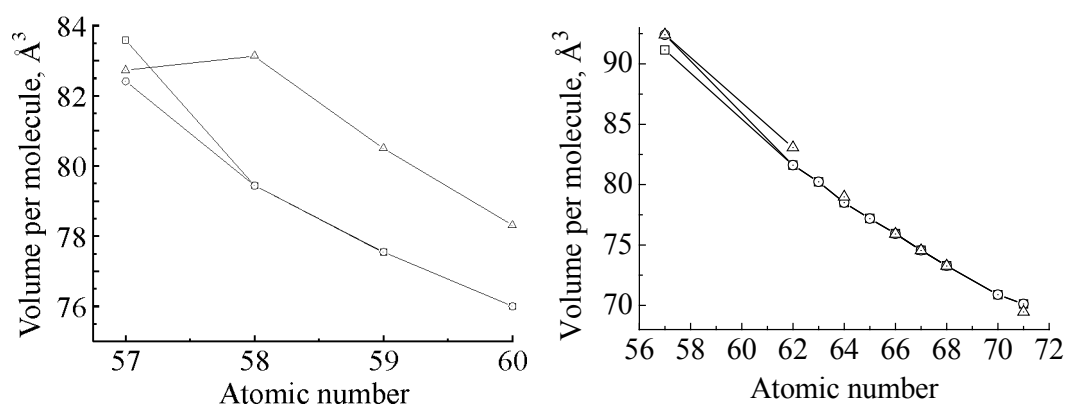


Fig. 1. Volume per molecule as a function of atomic number for *A*-type rare-earth sesquioxides calculated from atomic scale models: \square – this study, \circ – experiment [5–9], \triangle – *ab initio* [18]

Fig. 2. Volume per molecule as a function of atomic number for *C*-type rare-earth sesquioxides calculated from atomic scale models: \square – this study, \circ – experiment [5,13–17], \triangle – *ab initio* [18]

Table 2

Experimental data [10–12] for volumes, lattice parameters and angles of the *B*-type rare-earth sesquioxides

Parameters	Sm_2O_3	Eu_2O_3	Tb_2O_3
$V, \text{Å}^3$	149.722	146.945	141.917
$a, \text{Å}$	14.198	14.110	14.030
$b, \text{Å}$	3.627	3.602	3.536
$c, \text{Å}$	8.856	8.808	8.717
β, grad	99.986	100.037	100.100

For the *C*-type rare-earth sesquioxides there is complete agreement between the results of this study and the DFT and the experimental data. It is evident from Fig. 2 and Table 3 that the potential model reproduces accurately the crystal structure of both the *B*-type and *C*-type polymorphs, thus indicating the transferability of the model. For several *C*-type sesquioxides the DFT method employed by Hirosaki et al. [18] did not converge or was not feasible due to the absence of suitable pseudopotentials. Energy minimization techniques can bridge this gap by providing

Table 3

Atomistic computer simulation data for volumes, lattice parameters and angles of the B-type rare-earth sesquioxides

Parameters	Sm ₂ O ₃	Eu ₂ O ₃	Tb ₂ O ₃
$V, \text{Å}^3$	151.520	149.066	143.557
$a, \text{Å}$	14.383	14.311	14.143
$b, \text{Å}$	3.613	3.593	3.547
$c, \text{Å}$	8.898	8.848	8.737
β, grad	100.587	100.647	100.720

crystal structure data comparable to the experimental studies. It is evident from the results that the volume per molecule of the rare-earth oxides decreases with increasing atomic number regardless of their crystal structure. This is explained by the reduction of the rare-earth ionic radius with respect to the increase in atomic number (lanthanide contraction [33]).

3.2. Li⁺ Migration in Y₂O₃

The interstitial sites in the bixbyite structure form two paths. The 8*b* to 16*c* path was found to be more energetically favourable than the 16*c* to 24*d* path for the migration of lithium ions in Y₂O₃. To verify that the lithium ion follows a straight-line path from 8*b* to 16*c* a contour plot was generated representing the plane passing through the saddle point, perpendicular to the migration

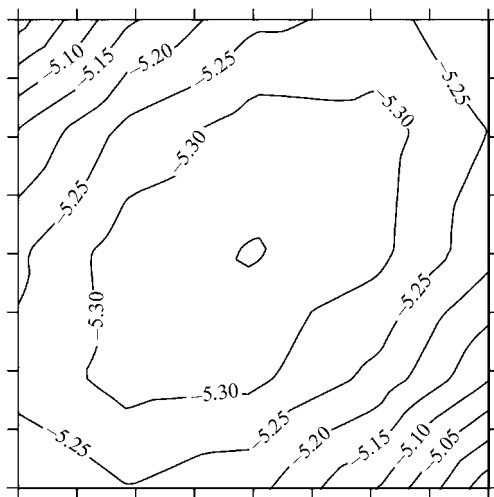


Fig. 3. Contour plot of the energy surface for a plane passing through the saddle point perpendicular to the migration vector containing the 16*c*–8*b* interstitial sites in Y₂O₃. The contour plot was obtained from positioning the lithium interstitial in 25 mesh points. The contour interval is 0.05 eV

vector (Fig. 3.). Fig. 3 is based on 25 calculations as the Li⁺ was positioned in an equidistant 5 × 5 grid in Y₂O₃. The lowest enthalpy point lies in the middle of the contour plot indicating that the lithium ion followed a straight-line path from interstitial site 8*b* to 16*c*.

Fig. 4 is a contour plot of the migration of Li⁺ interstitial in Y₂O₃, parallel to the migration vector containing the 16*c*–8*b*–16*c* interstitial site sequence. In this contour plot the Li⁺ was placed in a 21 × 21 grid and the 16*c*–8*b*–16*c* interstitial sites lie in the diagonal of the plot. The VI coordinate Li⁺ ion has an ionic radius of 0.76 Å whereas Y³⁺ has an ionic radius of 0.9 Å [34]. The lowest enthalpy sites are the interstitial sites and the lowest enthalpy path is the straight line connecting the 16*c*–8*b*–16*c* interstitial sites.

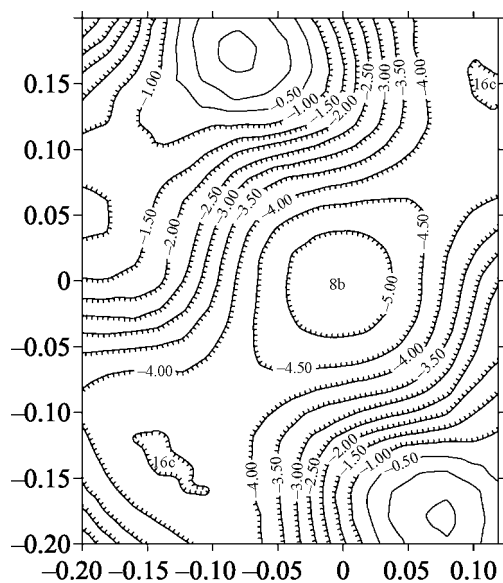


Fig. 4. Contour plot of the energy surface for a plane parallel to the migration vector containing the 16c–8b–16c interstitial site sequence in Y_2O_3 . The contour plot was obtained from positioning the lithium interstitial in 441 mesh points. The contour interval is 0.5 eV

As a fully ionic model was used and the calculations correspond to the dilute limit, the defect enthalpies will be over-estimated. Nevertheless, relative enthalpies are very reliable.

4. Conclusion

Atomic scale simulations adequately reproduce the 17 rare-earth oxides considered. This study provides a framework for further computational and structural studies. The derived short-range interatomic potential parameters can be used to systematically investigate the complex behaviour and defect chemistry of these materials at the atomic level. As such, we hope that the data presented here will encourage others to apply this model and develop new trends for rare-earth oxides and related compounds.

The authors gratefully acknowledge Prof. Robin Grimes and Dr Mark Levy of Imperial College London for useful conversations and Prof. Julian Gale of Curtin University for providing the GULP code.

1. M.H. Eder, G. Gritzner, *Supercond. Sci. Tech.* **18**, 87 (2005).
2. J.S. Wang, H.Y. Li, S. Yang, Y.Q. Liu, M.L. Zhou, *J. Alloys Comp.* **385**, 288 (2004).
3. R. Weber, J.A. Tanagerman, P.C. Nordine, R.N. Schennemann, K.J. Hiera, C.S. Ray, *J. Non-cryst. Solids* **345–346**, 359 (2004).
4. L.A. Kappers, R.H. Bartram, D.S. Hamilton, C. Brecher, A. Lempicki, *Nucl. Instr. Meth.* **A537**, 443 (2005).
5. H.R. Hoekstra, K.A. Gingerich, *Science* **146**, 1163 (1964).
6. O. Greis, R. Ziel, B. Breidenstein, A. Haase, T. Petzel, *J. Alloys Comp.* **216**, 255 (1994).
7. M. Faucher, J. Pannetier, Y. Charreire, P. Caro, *Acta Cryst.* **B38**, 344 (1982).
8. T. Atou, K. Kusaba, Y. Tsuchida, W. Utsumi, T. Yagi, Y. Suono, *J. Solid State Chem.* **38**, 288 (1981).
9. H. Baernighausen, G. Schiller, *Phase Transit.* **38**, 127 (1992).
10. H.L. Yakel, *Acta Cryst.* **B35**, 564 (1979).
11. T. Schleid, G. Meyer, *J. Less-Common Metals* **149**, 73 (1989).
12. E. Hubbert-Paletta, H. Mueller-Buschbaum, *Z. Anorg. Allg. Chem.* **363**, 145 (1968).
13. A. Bartos, K.P. Lieb, M. Uhrmacher, D. Wiarda, *Acta Cryst.* **B49**, 165 (1993).

14. Z.K. Heiba, Y. Akin, W. Sigmund, Y.S. Hascicek, J. Appl. Cryst. **36**, 1411 (2003).
15. A. Saiki, N. Ishizawa, N. Mizutani, M. Kato, Acta Cryst. **B40**, 76 (1984).
16. E.N. Maslen, V.A. Strel'tsov, N. Ishizawa, Acta Cryst. **B52**, 414 (1996).
17. Z. Heiba, H. Okuyucu, Y.S. Hascicek, J. Appl. Cryst. **35**, 577 (2002).
18. N. Hirotsuki, S. Ogata, C. Kocer, J. Alloys Comp. **351**, 31 (2003).
19. W.H. Zachariasen, Z. Phys. Chem. **123**, 134 (1926).
20. L. Pauling, Z. Kristallogr. **A69**, 415 (1928).
21. D.T. Cromer, J. Phys. Chem. **61**, 753 (1957).
22. G. Busker, A. Chroneos, R.W. Grimes, I.W. Chen, J. Am. Ceram. Soc. **82**, 1553 (1999).
23. R.W. Grimes, G. Busker, M.A. McCoy, A. Chroneos, J.A. Kilner, S.P. Chen, Ber. Bunsen. Phys. Chem. **101**, 1204 (1997).
24. R.W. Grimes, J. Alloys Comp. **279**, 75 (1998).
25. A. Chroneos, M.R. Levy, R.W. Grimes, C.R. Stanek, K.J. McClellan, Phys. Status Solidi **C** (in press).
26. A. Chroneos, K. Desai, S.E. Redfern, M.O. Zacate, R.W. Grimes, J. Mater. Sci. **41**, 675 (2006).
27. A. Chroneos, N. Ashley, K. Desai, J. F. Maguire, R.W. Grimes, J. Mater. Sci. (in press).
28. J.D. Gale, Faraday Trans. **93**, 629 (1997).
29. P.P. Ewald, Ann. Phys. **64**, 253 (1921).
30. B.G. Dick, A.W. Overhauser, Phys. Rev. **112**, 90 (1958).
31. N.F. Mott, M.J. Littleton, Trans. Faraday Soc. **34**, 485 (1938).
32. R.W.G. Wychoff, Crystal Structures, Interscience, New York (1964).
33. A.V. Prokofiev, A.I. Shelykh, B.T. Melekh, J. Alloys Comp. **242**, 41 (1996).
34. R.D. Shannon, Acta Cryst. **32**, 751 (1976).

A.I. Хронеос, Г. Баскер, І.Л. Гулатіс, Р.В. Вовк, А.А. Завгородній, М.О. Оболенський, О.Г. Петренко, В.М. Пінто Сімоес, О.В. Самойлов

АТОМІСТИЧНЕ МОДЕЛЮВАННЯ МІГРАЦІЇ Li^+ В Y_2O_3 І СТРУКТУРА СУПУТНІХ ОКСИДІВ

Атомістичні методи комп'ютерного моделювання, ґрунтовані на принципі мінімізації енергії, використані для прогнозування рівноважних параметрів і об'єма кристалічної ґратки ряду рідкоземельних оксидів та їх поліморф. Результати моделювання знаходяться в доброму узгодженні з експериментальними і літературними даними. Для демонстрації запропонованої обчислювальної методики розглянуто міграцію іонів літія (Li^+) в оксиді ітрія (Y_2O_3).

Ключові слова: атомістичне моделювання, кристалічна структура, міграція літія, рідкоземельні сполуки

*А.И. Хронеос, Г. Баскер, И.Л. Гулатис, Р.В. Вовк, А.А. Завгородний,
М.А. Оболенский, А.Г. Петренко, В.М. Пинто Симоэс, А.В. Самойлов*

АТОМИСТИЧЕСКОЕ МОДЕЛИРОВАНИЕ МИГРАЦИИ Li^+ В Y_2O_3 И СТРУКТУРА СОПУТСТВУЮЩИХ ОКСИДОВ

Атомистические методы компьютерного моделирования, основанные на принципе минимизации энергии, использованы для предсказания равновесных параметров и объема кристаллической решетки ряда редкоземельных оксидов и их полиморф. Результаты моделирования находятся в хорошем согласии с экспериментальными и литературными данными. Для демонстрации применимости предложенной вычислительной методики рассмотрена миграция ионов лития (Li^+) в оксиде иттрия (Y_2O_3).

Ключевые слова: атомистическое моделирование, кристаллическая структура, миграция лития, редкоземельные соединения